PERGAMON

International Journal of Heat and Mass Transfer 44 (2001) 2005–2009

International Journal of HEAT and MASS TRANSFER

www.elsevier.com/locate/ijhmt

Technical Note

Film cooling subject to bulk flow pulsations: effects of density ratio, hole length-to-diameter ratio, and pulsation frequency

P.M. Ligrani *, C.M. Bell [1]

Convective Heat Transfer Laboratory, Department of Mechanical Engineering, University of Utah, Salt Lake City, UT 84112, USA

Received 23 September 1999; received in revised form 7 July 2000

1. Introduction

Investigations of arrays of turbine blades placed in linear cascades show that the unsteadiness from the relative motion of adjacent blade rows produces greater reductions to film cooling protection on suction surfaces than on pressure surfaces [1,2]. A number of other recent studies present experimental data or numerical predictions which further illustrate the dramatic effects of unsteadiness due to potential flow interactions and passing shock wave families on cooling films [3–15]. The present study examines the effects of variations of static pressure and streamwise velocity imposed throughout a turbulent boundary layer film cooled with a single row of simple angle film cooling holes. The experimental test conditions thus model the same modes of unsteadiness that are imposed near turbine airfoil surfaces from potential flow interactions and passing families of oblique shock waves.

Bulk flow pulsations, in the form of sinusoidal variations of static pressure and streamwise velocity, are shown to have important influences on film cooling from round, simple-angle holes in a turbulent boundary layer when the time-averaged blowing ratio $\bar{m}$ is 0.7. Distributions of adiabatic film cooling effectiveness $\bar{\eta}$, and overall film cooling performance parameter $\dot{q}''/\dot{q}_0''$ are both altered by the pulsations. The protection nominally provided by the film cooling decreases by important amounts as imposed pulsation frequency n increases at constant density ratio ρ_c/ρ_∞. Changes with l/d depend upon magnitudes of ρ_c/ρ_∞ and n. The parameter whose changes have the largest effect is n, followed by ρ_c/ρ_∞, and then l/d. Investigated are $\bar{u}_\infty$ of 10 m/s, $\bar{m}$ of 0.7, l/d of 3 and 4, n equal to 0, 8, and 20 Hz, and ρ_c/ρ_∞ of 0.94, 1.20–1.25, and 1.36–1.40. Ranges of other parameters are: $Re_d = 2800$–6800, $Re = 578\,000$–$1\,100\,000$, $Sr_c =$ 0–2.3, and $Sr_\infty = 0$–0.6. Because density ratios here range from 0.9 to 1.4, the experimental conditions employed are different from ones covered in previous investigations [7–15], where ρ_c/ρ_∞ values near 1 are employed. Higher density ratio values are investigated because of their use in operating turbines of gas turbine engines.

2. Experimental apparatus and procedures

The wind tunnel, experimental apparatus, film cooling injectant system, procedures for measuring local adiabatic film cooling effectiveness, procedures for measuring magnitudes of the overall film cooling performance parameter, and procedures for generating bulk flow pulsations are given by Bell et al. [15].

The experimental uncertainty of $\bar{\eta}$ is about ±5.5%. The experimental uncertainty of $\dot{q}''/\dot{q}_0''$ ranges from ±3.0% to ±8.0%. Additional details are provided by Bell [14].

3. Experimental results and discussion

Experimental conditions: Injectant, freestream, and pulsation experimental conditions are summarized in Table 1. Injection Reynolds number $d\bar{u}_c/\nu$ ranges from about 2800 to about 5000, which are high enough to insure that turbulent flow is present at the injection hole exits.

Baseline data comparisons: The present measurements downstream of $l/d = 4$ holes (with no pulsations) compare favorably with results from Pedersen et al. [16] at

* Corresponding author. Tel.: +1-801-581-4240; fax: +1-801-585-9826.

E-mail address: ligrani@mech.utah.edu (P.M. Ligrani).

[1] Present address: Raytheon Corporation, Tucson, AZ.

PII: S0017-9310(00)00249-0

Nomenclature

d	injection hole diameter
I	momentum flux ratio
l	injection hole length
$\bar{m}$	time-averaged blowing ratio, $\rho_c \bar{u}_c / \rho_\infty \bar{u}_\infty$
n	pulsation frequency
$\dot{q}_0''$	surface heat flux with no film cooling
$\dot{q}''$	spanwise-averaged surface heat flux with film cooling
Re_d	coolant Reynolds number, $d\bar{u}_c/v$
Re	freestream Reynolds number, $X\bar{u}_\infty/v$
Sr_c	coolant Strouhal number, $2\pi n l/\bar{u}_c$
Sr_∞	freestream Strouhal number, $2\pi n\delta/\bar{u}_\infty$
Sr	modified Strouhal number, $Sr_c/[\bar{m}^{0.6}(\rho_c\rho_\infty)^{2.0}(l/d)^{2.0}]$
T	temperature
$\bar{T}$	spanwise-averaged temperature
$\bar{u}_\infty$	time-averaged freestream velocity
$\bar{u}_c$	time-averaged and spatially-averaged injectant velocity
x	streamwise coordinate measured from downstream edge of film cooling holes
X	streamwise coordinate measured from boundary layer trip
z	spanwise coordinate measured from spanwise centerline of test surface

Greek symbols

η	local film cooling effectiveness, $(T_{aw} - T_\infty)/(T_c - T_\infty)$
$\bar{\eta}$	spanwise-averaged film cooling effectiveness, $(\overline{T_{aw}} - T_\infty)/(T_c - T_\infty)$
ρ	density

Subscripts

aw	adiabatic wall value
c	injectant or coolant
∞	freestream
w	wall value

Table 1
Injectant, freestream, and pulsation experimental conditions

$\bar{m}$	ρ_c/ρ_∞	$\bar{u}_c/\bar{u}_\infty$	I	l/d	n (Hz)	Sr_c	Sr
0.67	0.94	0.71	0.475	3	0	0	0
0.67	0.94	0.71	0.477	3	8	0.47	0.075
0.67	0.94	0.71	0.477	3	20	1.18	0.189
0.68	1.25	0.54	0.364	3	0	0	0
0.68	1.24	0.55	0.369	3	8	0.61	0.056
0.67	1.19	0.57	0.385	3	20	1.47	0.147
0.66	1.39	0.48	0.318	3	0	0	0
0.67	1.40	0.48	0.319	3	8	0.70	0.050
0.67	1.36	0.49	0.326	3	20	1.71	0.131
0.68	0.94	0.72	0.487	4	0	0	0
0.67	0.94	0.71	0.474	4	8	0.63	0.057
0.67	0.94	0.71	0.474	4	20	1.57	0.141
0.68	1.28	0.53	0.36	4	0	0	0
0.67	1.26	0.53	0.354	4	8	0.84	0.042
0.68	1.25	0.54	0.365	4	20	2.07	0.104
0.67	1.40	0.48	0.323	4	0	0	0
0.67	1.40	0.48	0.323	4	8	0.93	0.038
0.66	1.38	0.48	0.318	4	20	2.32	0.098

about the same density ratios, even though film-hole geometry and flow conditions are slightly different in the two studies.

Adiabatic film cooling effectiveness: Fig. 1 presents spanwise-averaged film cooling effectiveness values for different x/d, different l/d, different imposed pulsation frequencies, and different density ratios for $\bar{m} = 0.7$. Data in the three parts of the figure are given for pulsation frequencies n of 0, 8 and 20 Hz, respectively. The data are presented to illustrate the changes which occur as density ratio increases as blowing ratio $\bar{m}$ is held constant. When compared at the same $\bar{m}$, x/d, l/d, and n, spanwise-averaged effectiveness data generally increase with ρ_c/ρ_∞. One major exception is evident when $l/d = 3$ and $n = 20$ Hz, where *portions* of the $\rho_c/\rho_\infty = 0.94$ data are higher than data measured at ρ_c/ρ_∞ of 1.20–1.25 and 1.36–1.4. Increases in effectiveness with ρ_c/ρ_∞ are generally more evident at x/d values less than 24.5, and the largest changes of $\bar{\eta}$ due to ρ_c/ρ_∞ are apparent at a flow pulsation frequency of 0 Hz.

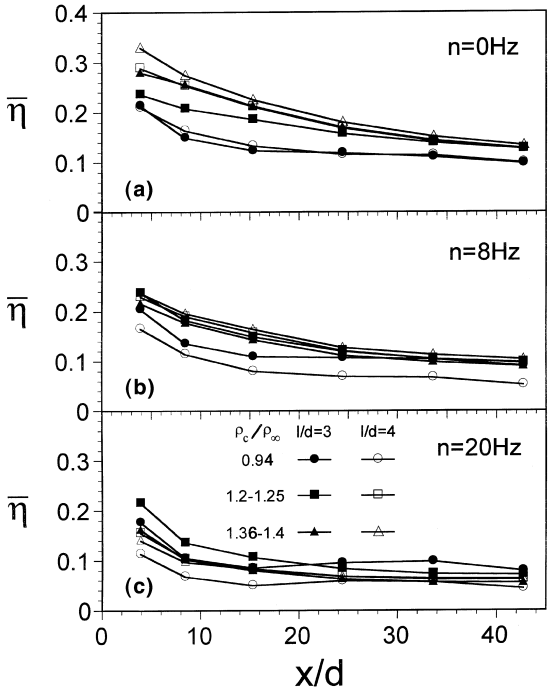

Fig. 1. Spanwise-averaged adiabatic film cooling effectiveness variations with x/d, l/d, and density ratio ρ_c/ρ_∞ at different imposed pulsation frequencies for $\bar{m} = 0.7$: (a) $n = 0$ Hz; (b) $n = 8$ Hz; (c) $n = 20$ Hz.

Changes of $\overline{\eta}$ with ρ_c/ρ_∞ are then smaller at higher frequencies, and the smallest effectiveness increases with ρ_c/ρ_∞ are present at a pulsation frequency of 20 Hz. This is mostly due to changes to *time-averaged* film concentration positions produced by the flow pulsations at this frequency. A pulsation frequency of 20 Hz also causes the injectant to be non-quasi-steady [7]. As a result, the whole film trajectory lifts-off the test surface in a wavy manner, and greater reductions in protection and overall film cooling performance are present than when the film is quasi-steady [8,10,12].

When data in the three parts of Fig. 1 are compared, it is evident that spanwise-averaged effectiveness data consistently decrease as the imposed pulsation frequency increases when compared at the same $\bar{m}$, x/d, l/d, and ρ_c/ρ_∞. These effectiveness decreases become larger and significantly more pronounced as the density ratio becomes larger. Density ratios ρ_c/ρ_∞ of 0.94, 1.20–1.25, and 1.36–1.4 correspond to momentum flux ratios of 0.48–0.49, 0.36–0.39, and 0.32–0.33, respectively. The data in Fig. 1 show that the film at the lowest of these momentum flux ratios (0.32–0.33) is most affected by the pulsations (as ρ_c/ρ_∞ is held constant). This is because the time-averaged position of the film is often moved farther from the wall as pulsation frequency increases. This occurs because periodically varying static pressure at the film hole exits results in periodic variations in film mass flux, blowing ratio, momentum flux, and film trajectory [7]. When static pressure is low, the instantaneous film momentum flux is high, the instantaneous film trajectory is farther from the surface, and the flow-away from the film is swept to regions near the surface beneath the film to decrease protection. The opposite trend occurs during each pulsation when the static pressure is high [7,12]. The net effect is a periodic decrease in protection, which translates into a *time-averaged* decrease in protection and lower spanwise-averaged effectiveness values.

Overall film cooling performance parameter: Overall film cooling performance at a particular location on a turbine surface is given by $\dot{q}''/\dot{q}_0''$, the ratio of the heat flux with film cooling to the heat flux with no film cooling. Lower values indicate better film cooling protection. Procedures for determining $\dot{q}''/\dot{q}_0''$ are given by Bell et al. [15], and rely on measurement of the isoenergetic Stanton number ratio data, also given by Bell et al. [15] for $\rho_c/\rho_\infty = 1.00$.

Fig. 2 shows how spanwise-averaged film cooling performance parameters vary with normalized streamwise distance x/d, hole length-to-diameter ratio l/d, and imposed pulsation frequency n, for $\bar{m} = 0.7$. The three parts of the figure represent ρ_c/ρ_∞ of 0.94, 1.20–1.25, and 1.36–1.4, respectively. From Fig. 2, it is evident that: (i) the lowest $\dot{q}''/\dot{q}_0''$ magnitudes and best film cooling

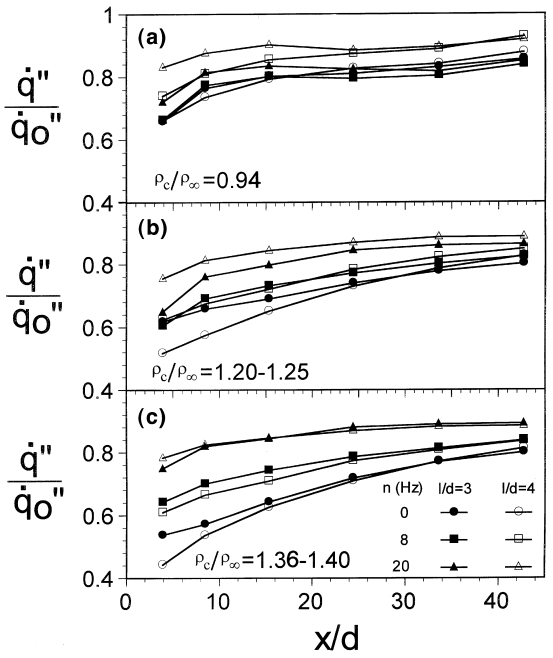

Fig. 2. Spanwise-averaged performance parameter variations with x/d, l/d, and imposed pulsation frequency n at different density ratios for $\bar{m} = 0.7$: (a) $\rho_c/\rho_\infty = 0.94$; (b) $\rho_c/\rho_\infty = 1.20$–$1.25$; (c) $\rho_c/\rho_\infty = 1.36$–$1.40$.

protection over the widest ranges of x/d are generally present when $n = 0$ Hz and no pulsations are imposed, (ii) protection generally degrades at each x/d as imposed pulsation frequency n increases, and (iii) protection changes with increasing pulsation frequency become larger and significantly more pronounced as the density ratio becomes larger. One exception to these trends is evident for $\rho_c/\rho_\infty = 0.94$, where differences between the $\dot{q}''/\dot{q}_0''$ data at different n are quite small when $l/d = 3$.

The increased influences of pulsations at higher density ratios are due to the variations of density between the film and the surrounding boundary layer and free-stream. With no pulsations imposed upon the flow, protection generally improves as the ρ_c/ρ_∞ density ratio increases at given values of pulsation frequency n, blowing ratio $\bar{m}$, and x/d location. The same trend is also often present when pulsations are present. This is because of the action of the pulsations in changing the positions of the highest film concentrations periodically with time. The result is larger differences in protection as the film moves, which results in a larger time-variation of protection over each imposed pulsation cycle. This then leads to greater changes in time-averaged protection as the pulsation frequency varies.

When $\rho_c/\rho_\infty = 1.36$–$1.4$, Fig. 2 additionally shows that slightly better protection is generally present when $l/d = 4$ compared to $l/d = 3$ (for each x/d at all pulsation frequencies). The opposite trend with l/d is generally evident for the $\rho_c/\rho_\infty = 0.94$ data. When $\rho_c/\rho_\infty = 1.20$–$1.25$, protection improves as l/d changes from 3 to 4 when $n = 0$ Hz, stays about the same when $n = 8$ Hz, and degrades when $n = 20$ Hz. Performance parameters in Fig. 2 thus show different trends as l/d changes from 3 to 4, which depend upon the magnitudes of the pulsation frequency n and density ratio ρ_c/ρ_∞. As such, $\dot{q}''/\dot{q}_0''$ trends are qualitatively similar to variations of $\overline{\eta}$ with these parameters [14]. Such behavior illustrates the complexity and non-linearity of boundary layers with high density ratio films when bulk flow pulsations are imposed.

Fig. 3 illustrates the influences of increasing density ratio on magnitudes of the overall film cooling performance parameter for $\bar{m} = 0.7$. Variations with x/d and l/d are also evident. Data in the three parts of the figure correspond to pulsation frequencies n of 0, 8, and 20 Hz, respectively. The data generally show increases in protection (and lower $\dot{q}''/\dot{q}_0''$ values), which are present at most x/d, as density ratio increases. The most notable exception is evident when $l/d = 3$ and $n = 20$ Hz, where portions of the $\rho_c/\rho_\infty = 0.94$ data evidence better protection than data measured at ρ_c/ρ_∞ of 1.20–1.25 and 1.36–1.40.

Overall data trends: The present results show that higher density ratios give lower coolant Strouhal numbers, which means that increasing coolant Strouhal number Sr_c does not necessarily correspond to degraded

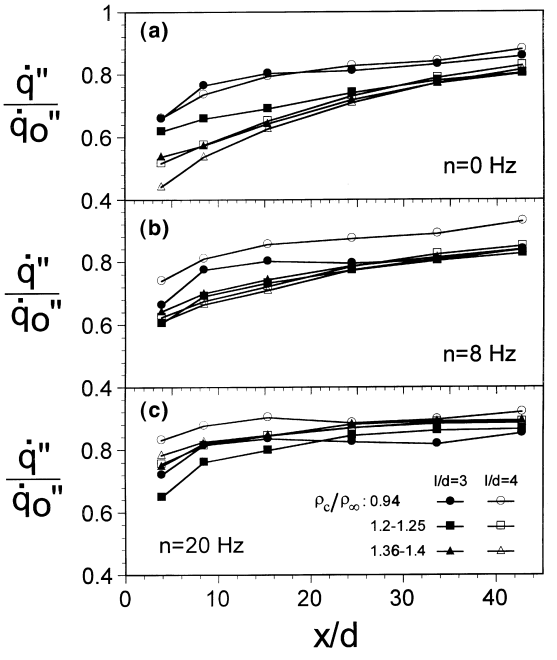

Fig. 3. Spanwise-averaged performance parameter variations with x/d, l/d, and density ratio ρ_c/ρ_∞ at different imposed pulsation frequencies for $\bar{m} = 0.7$: (a) $n = 0$ Hz; (b) $n = 8$ Hz; (c) $n = 20$ Hz.

protection [7,8,12]. A modified Strouhal number, Sr, is needed to characterize the reductions in the protection which occur as pulsations imposed on film cooled boundary layers. Such reductions are present when

$$Sr = Sr_c/[\bar{m}^{0.6}(\rho_c/\rho_\infty)^{2.0}(l/d)^{2.0}] > C, \quad (1)$$

where $C = 0.055$–0.070. Magnitudes of Sr and Sr_c are given in Table 1. Eq. (1) may be rearranged to become

$$Sr_c > C\bar{m}^{0.6}(\rho_c/\rho_\infty)^{2.0}(l/d)^{2.0}. \quad (2)$$

These equations not only provide a good match to the present experimental data, but they are also consistent with results given by Ligrani et al. [7–10], Jung and Lee [13], and Seo et al. [6,12] for l/d of 1.6, 4, and 10. In contrast to the present data, those data are obtained for ρ_c/ρ_∞ only in the vicinity of 1.

According to the data presented, alterations in protection due to increasing pulsation frequency become more significant as the density ratio ρ_c/ρ_∞ becomes larger. At given values of pulsation frequency n, blowing ratio $\bar{m}$, and x/d location, protection generally improves as the ρ_c/ρ_∞ density ratio increases. Thus, pulsation frequency and density ratio have opposite influences on the protection provided by film cooling in turbulent boundary layers. These competing influences are included in correlation Eqs. (1) and (2) above, which show acceptable levels of protection ($\dot{q}''/\dot{q}_0'' < 0.7$ at $x/d < 10$)

over wider ranges of imposed pulsation frequency n as ρ_c/ρ_∞ becomes larger.

Acknowledgements

This effort is sponsored by the National Science Foundation, Grant number CTS-9615196.

References

[1] M.J. Rigby, A.B. Johnson, M.L.G. Oldfield, Gas turbine rotor blade film cooling with and without simulated NGV shock waves and wakes, Paper No. 90-GT-78, in: International Gas Turbine and Aeroengine Congress and Exposition, Brussels, 1990.

[2] R.S. Abhari, A.H. Epstein, An experimental study of film cooling in a rotating transonic turbine, ASME Trans.—J. Turbomachinery 116 (1994) 63–70.

[3] K.A. Juhany, M.L. Hunt, Flowfield measurements in supersonic film cooling including effect of shock-wave interaction, AIAA J. 32 (1994) 578–585.

[4] T. Kanda, F. Ono, M. Takahashi, T. Saito, Y. Wakamatsu, Experimental studies of supersonic film cooling with shock wave interaction, AIAA J. 34 (1996) 265–271.

[5] R.S. Abhari, Impact of rotor-stator interaction on turbine blade film cooling, ASME Trans.—J. Turbomachinery 118 (1996) 103–113.

[6] H.J. Seo, J.S. Lee, P.M. Ligrani, The effect of injection hole length on film cooling with bulk flow pulsations, Int. J. Heat Mass Transfer 41 (1998) 3515–3528.

[7] P.M. Ligrani, R. Gong, J.M. Cuthrell, J.S. Lee, Bulk flow pulsations and film cooling—I. Injectant behavior, Int. J. Heat Mass Transfer 39 (1996) 2271–2282.

[8] P.M. Ligrani, R. Gong, J.M. Cuthrell, J.S. Lee, Bulk flow pulsations and film cooling—II. Flow structure and film effectiveness, Int. J. Heat Mass Transfer 39 (1996) 2283–2292.

[9] P.M. Ligrani, R. Gong, J.M. Cuthrell, J.S. Lee, Effects of bulk flow pulsations on film-cooled boundary layer structure, ASME Trans.—J. Fluids Eng. 119 (1997) 56–66.

[10] P.M. Ligrani, R. Gong, J.M. Cuthrell, Bulk flow pulsations and film cooling: flow structure just downstream of the holes, ASME Trans.—J. Turbomachinery 119 (1997) 568–573.

[11] D.K. Sohn, J.S. Lee, The effects of bulk flow pulsations on film cooling from two rows of holes, Paper No. 97-GT-129, in: International Gas Turbine and Aeroengine Congress and Exposition, Orlando, 1997.

[12] H.J. Seo, J.S. Lee, P.M. Ligrani, Effects of bulk flow pulsations on film cooling from different length injection holes at different blowing ratios, Paper No. 98-GT-192, in: International Gas Turbine and Aeroengine Congress and Exposition, Stockholm, 1998.

[13] I.-S. Jung, J.S. Lee, Effects of bulk flow pulsations on film cooling from spanwise oriented holes, Paper No. 98-GT-211, in: International Gas Turbine and Aeroengine Congress and Exposition, Stockholm, 1998.

[14] C.M. Bell, Effects of bulk flow pulsations on film cooling with different density ratios, Master of Science thesis, University of Utah, 1998.

[15] C.M. Bell, P.M. Ligrani, W.A. Hull, C.M. Norton, Film cooling subject to bulk flow pulsations: effects of blowing ratio freestream velocity and pulsation frequency, Int. J. Heat Mass Transfer 42 (23) (1999) 4333–4344.

[16] D.R. Pedersen, E.R.G. Eckert, R.J. Goldstein, Film cooling with large density differences between the mainstream and the secondary fluid measured by the heat–mass transfer analogy, ASME Trans.—J. Heat Transfer 99 (1977) 620–627.